Anomalous Conductance Quantization in Carbon Nanotubes

M. J. Biercuk, N. Mason, J. Martin,* A. Yacoby,* and C. M. Marcus
Department of Physics, Harvard University, Cambridge, Massachusetts 02138, USA
(Received 25 June 2004; published 18 January 2005)

Conductance measurements of carbon nanotubes containing gated local depletion regions exhibit plateaus as a function of gate voltage, spaced by approximately $1e^2/h$, the quantum of conductance for a single (nondegenerate) mode. Plateau structure is investigated as a function of bias voltage, temperature, and magnetic field. We speculate on the origin of this surprising quantization, which appears to lack band and spin degeneracy.

DOI: 10.1103/PhysRevLett.94.026801 PACS numbers: 73.63.Fg

Carbon nanotubes free of disorder are expected to behave as ideal quantum wires with electrical conduction occurring through one-dimensional (1D) modes [1], each with conductance quantized in units of e^2/h. In a variety of physical systems, including gate-defined quantum point contacts [2] and cleaved-edge wires [3], such 1D behavior appears as conductance plateaus as a function of voltage on nearby gates, which act to reduce density in the wire and hence depopulate 1D modes. In gated heterostructure quantum point contacts, conductance steps of $2e^2/h$ are observed, the factor of 2 reflecting spin degeneracy of the subbands [4,5]. By analogy, one would expect nanotubes to show either a single step of $4e^2/h$, reflecting the four modes per subband associated with spin and band degeneracy [6,7], or two steps spaced by $2e^2/h$ if band degeneracy were lifted, for instance by strain [7]. In this Letter we report conductance plateaus in gated nanotube devices in various configurations, revealing an unexpected plateau spacing of $\sim 1e^2/h$ at zero applied magnetic field.

Conductance quantization has previously been observed in multiwalled carbon nanotubes by immersing one end in a liquid conductor [8]. This study found quantization principally in units of $2e^2/h$, with additional plateaus appearing near e^2/h under certain conditions. In single-walled nanotubes, multiple steps in dc current were reported in devices with highly resistive metal contacts [9,10] and were attributed to populating higher 1D subbands.

The nanotubes used in this study were grown by chemical vapor deposition (CVD) from Fe catalyst on doped Si wafers (which serve as back gates) with 1 μm thermal SiO_2 and contacted with $\sim$15 nm of Pd [11]. All measured devices had nanotube diameters in the range $\sim$1.5–5 nm (actual diameters noted in figure captions) [12]. In some cases, the nanotubes were pushed with the tip of an atomic force microscope (AFM) to form a bend [13–15]. Three device configurations were investigated: bent tubes with side gates [Fig. 1(b), inset], as well as unbent and bent tubes with local electrostatic top-gates [Fig. 3(a), inset]. It has previously been shown that bends create gate-depletable regions [14,15], and that local gates affect only proximal sections of the tube [16]. The top-gated devices were made by depositing CVD-grown SiO_2 on the Pd-contacted nanotubes and patterning Cr/Au gates using electron-beam lithography [16,17]. Two-terminal differential conductance, $G = dI/dV$, was measured as a function of source-drain bias, V_{SD}, by applying dc + ac voltage, $V = V_{SD} + V_{ac}$ (with $V_{ac} \sim 50$–180 μV), and separately measuring dc and ac currents. Fourteen devices in these configurations showed qualitatively similar behavior.

Figure 1(a) shows characteristic plateau features in dI/dV for an intentionally bent tube [device shown in Fig. 1(b)] as a function of source-drain voltage, V_{SD}, with the voltage on a local side gate near the bend, V_{SG}, held fixed for each trace. Plateaus appear as bunched traces where the conductance changes little as V_{SG} is changed. These plateaus are also apparent in slices taken at fixed V_{SD} [colored vertical lines in Fig. 1(a)] as a function of V_{SG}, as shown in Fig. 1(b). In this device, high-bias dI/dV saturates at $\sim 3.3e^2/h$, somewhat below the ideal value of $4e^2/h$, presumably due to backscattering at the contacts or within the tube. To account for this, a series resistance, R_S, is subtracted to bring the high-field saturation to $\sim 4e^2/h$. Several plateaus are visible, at both low and high bias ($V_{SD} \sim 30$ mV), spaced by roughly e^2/h. Plateaus around zero bias show considerable overshoot, while those at high bias are typically much flatter. Smooth evolution between these two sets of plateaus with changing V_{SD} is also evident, and revealed more clearly in Fig. 2. Conductance shows a dip around zero bias that deepens as temperature is lowered. Further, near $V_{SD} = 0$ at temperatures below $\sim$15 K, single-electron charging is evident when the conductance is below the first plateau [Fig. 1(c)], while in the high conductance region, a Fabry-Perot-like interference pattern is observed [Fig. 1(d)] [18]. Irregularity in the interference pattern may be due to scattering from intrinsic defects in the nanotube, but the persistence of Fabry-Perot interference implies that this scattering does not significantly affect ballistic transport in the device. The Fabry-Perot structure and the zero bias dip may affect the positions of the plateaus, especially near $V_{SD} = 0$.

The transconductance, dG/dV_{SG}, for the same device [inset Fig. 1(b)] is shown in Fig. 2(a). Transconductance

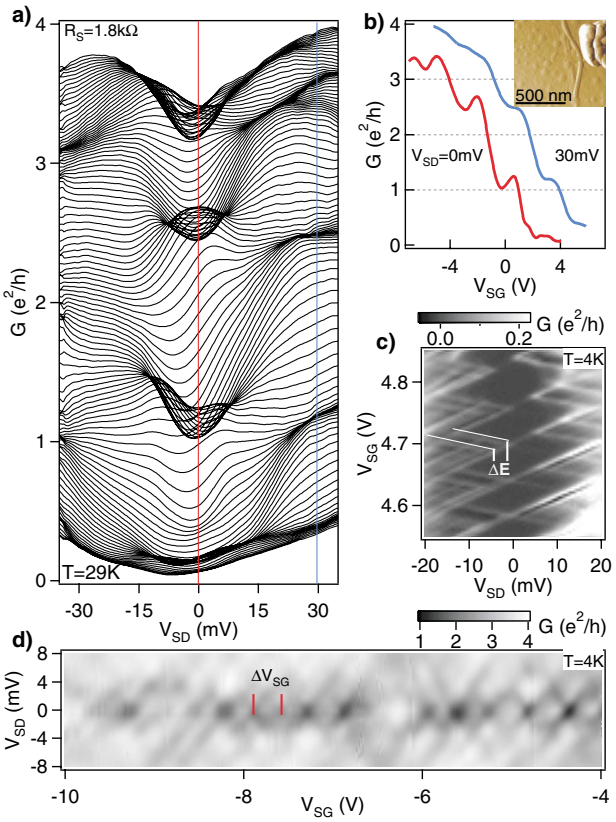

FIG. 1 (color). (a) Differential conductance $G = dI/dV$ as a function of source-drain bias, V_{SD}, and side gate voltage, V_{SG}, for a bent nanotube device, diameter $d \sim 3.5$ nm, at temperature $T = 29$ K. Series resistance R_S is indicated. Traces are taken at fixed V_{SG}; bunched traces correspond to conductance plateaus. (b) Slices from (a) at fixed V_{SD}. The high-bias trace is offset by 2 V in V_{SG} for clarity. Inset: AFM image of the device, showing a tube pushed toward the side gate (top right). Total device length is ~1.5 μm. (c) G measured at 4 K for the same device with V_{SG} set below the first plateau where Coulomb blockade diamonds are evident. Typical excited state level spacings, ΔE, are 2–3 meV, corresponding to a device length $L \sim 500$–700 nm. (d) G in the high conductance region ($G > e^2/h$), with Fabry-Perot interference period $\Delta V_{SG} \sim 0.3$ V. For this panel, series resistance $R_S = 1.2$ kΩ.

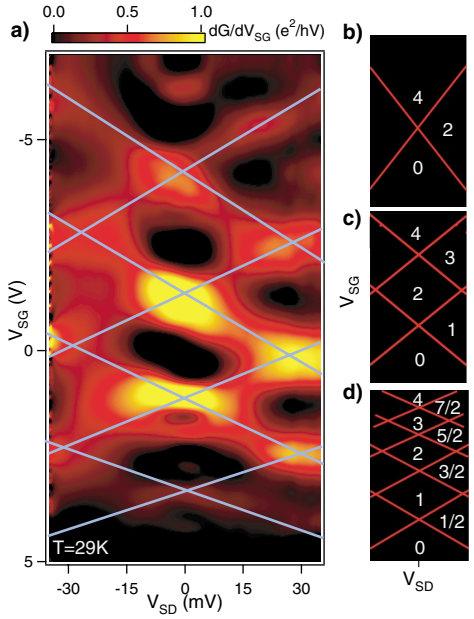

FIG. 2 (color). (a) Transconductance, dG/dV_{SG} as a function of V_{SD} and V_{SG} for data in Fig. 1(a). Dark regions correspond to plateaus, bright regions to transitions between plateaus. Blue lines are guides indicating the evolution of conductance modes with V_{SD} and V_{SG}. (b)–(d) Models for transconductance evolution with gate voltage for a four-mode 1D conductor for the case of (b) fourfold degeneracy, (c) two-fold degeneracy, and (d) fully broken degeneracy. Numbers denote expected conductance values for plateaus in units of e^2/h (see text).

highlights transitions between plateaus as bright regions, with dark regions representing the plateaus. Figure 2(a) shows that as $|V_{SD}|$ is increased, each transition splits into two which at larger bias recross, restoring the original number of plateaus. [It is near this recrossing value of bias, $V_{SD} \sim 30$ mV, that the high-bias cut in Fig. 1(b) is taken.] The resulting pattern of transitions can be interpreted in the context of transport through quantized modes: if one assumes that each transition corresponds to the entering of a 1D mode into the transport window, then the diamond pattern in dG/dV_{SG} follows the evolution of mode energies with V_{SD} and V_{SG}. This is the standard noninteracting picture of nonlinear "half plateaus" in quantum point contacts [19,20].

Experimental dG/dV_{SG} [Fig. 2(a)] can be compared to various schemes for the evolution of 1D modes. In the simplest picture of four conduction modes with spin and band degeneracy [21], one expects a single transition from $G = 0$ to $G = 4e^2/h$ around zero bias as V_{SG} is increased, and a single half plateau with $G = 2e^2/h$ at high bias [Fig. 2(b)]. With one degeneracy lifted (e.g., band degeneracy lifted by strain), the simple picture gives features as in Fig. 2(c), with plateaus and half plateaus spaced by $2e^2/h$. With all degeneracies lifted, this picture gives four plateaus and four transitions each spaced by e^2/h, and half plateaus at $1/2$, $3/2$, $5/2$, and $7/2$ times e^2/h [Fig. 2(d)]. Surprisingly, the experimental data most resemble the schematic in Fig. 2(d).

Within an interpretation of separate 1D modes, positions of the half plateaus from Fig. 2(a) give a value for the 1D-mode energy spacing of $\Delta_{1D} \sim 55$ meV between the first and the second plateau, with a spacing in $V_{SG} \sim 1.8$ V. Together, these give a coupling efficiency $\alpha \equiv \delta E/e\delta V_{SG} \sim 0.03$, which describes the shift of the Fermi level in the nanotube with V_{SG} [22]. The coefficient $\alpha = C_L/(e^2\partial n/\partial\mu)$, where $C_L^{-1} = (C_L^G)^{-1} + (e^2\partial n/\partial\mu)^{-1}$, contains both a geometrical capacitance per unit length, C_L^G, and a term reflecting the kinetic energy (per unit length) required to increase the depth of the Fermi sea (n is the linear density and μ is the chemical potential). Since $\alpha \ll 1$ (kinetic capacitance dominates geometric), we may approximate $\alpha \sim C_L^G/(e^2\partial n/\partial\mu)$. The kinetic component can be calculated from a linear dispersion relation,

$\delta E = \hbar v_F \delta k$ and $\delta k = \pi \delta n / M$ (where M is the number of modes), giving $e^2 \partial n / \partial \mu = e^2 / \pi \hbar v_F \sim 100$ pF/m per mode, where $v_F \sim 8 \times 10^5$ m/s is the typical Fermi velocity. The measured value $\alpha \sim 0.03$, extracted when only one mode is present, can then be used to calculate $C_L^G \sim 3$ pF/m.

The estimate of C_L^G above has assumed fully lifted degeneracies. This interpretation is supported by a comparison of the length of the mechanical bend (~500 nm) with the effective device length L associated with both Coulomb blockade and Fabry-Perot oscillations, determined using C_L^G. The period of Coulomb blockade oscillations, $\Delta V_{SG} = e(LC_L^G)^{-1} \sim 0.05$ V, which corresponds to the addition of one electron to a length L, gives $L \sim 1$ μm. The period in V_{SG} of the Fabry-Perot pattern corresponds to a change in wave vector by $\delta k_F = \pi / L$, hence a change in carrier density by $\delta n = 4 \delta k_F / \pi$, taking all modes to be occupied near the highest plateau, where Fabry-Perot is measured. Relating the Fabry-Perot period $\Delta V_{SG} = 0.3$ V to density, $e \delta n = C_L^G \Delta V_{SG}$, gives an independent estimate of effective device length, $L = 4e(\Delta V_{SG} C_L^G)^{-1} \sim 700$ nm, using C_L^G from above.

We note that interpreting the measured half-plateau positions in terms of 1D subbands would require a nanotube diameter of ~15 nm, inconsistent with AFM measurements for all devices. If the band structure of the nanotube were modified substantially by the presence of a mechanical defect and a nonuniform gate, the 1D subband spacing could be reduced to the values we observe [23]. However, the appearance of plateaus spaced by e^2/h is not to our mind explained by the influence of defects, nor by other structures such as multiple nanotube shells.

In all measured devices, dI/dV was everywhere less than $4e^2/h$. Subtracting R_S to bring the large-bias conductance to $4e^2/h$ typically yielded plateaus and half plateaus spaced by $\sim e^2/h$ [24]. In no case could we subtract an appropriate R_S to give plateaus separated by $2e^2/h$ or $4e^2/h$.

Figure 3 demonstrates the effect of the gates in producing spatially localized depletion regions. Conductance of an unbent tube with two top gates shows plateau structure as a function of either gate. The two gates evidently act independently, each depleting different regions of the tube, leading to the square pattern seen in the inset of Fig. 3(a). Two gates influencing the same region of the tube would produce a diagonal pattern instead.

Three of the measured devices showed a nonconductive region as a function of gate voltage with high conductance regions on either side, presumably reflecting an energy gap in a semiconducting nanotube [25]. Data for one such device, an intentionally bent tube without local gates, are shown in Fig. 3(b). Both the holelike regime (at negative gate voltage), and the electronlike regime (at positive gate voltage) show e^2/h conductance plateaus as a function of gate voltage. Figure 3(c) shows plateau structure with spacings of $\sim e^2/h$ in another bent-tube device as a function of top gate voltage over the bend and V_{SD}.

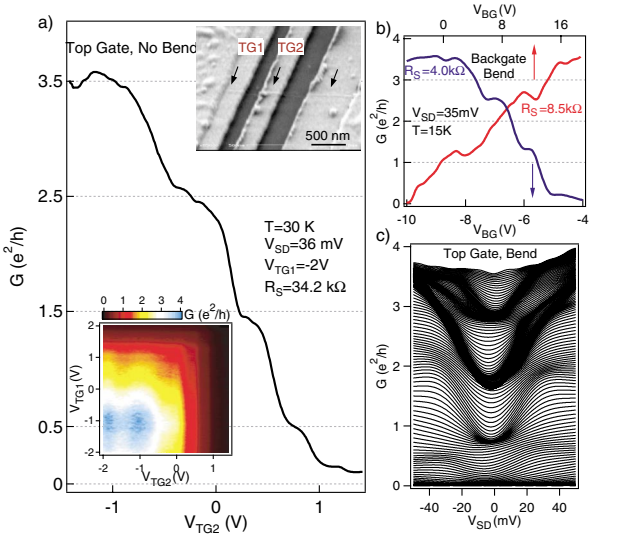

FIG. 3 (color). (a) Differential conductance G as a function of gate voltage for an unbent nanotube, $d \sim 1.5$ nm, with top gates, showing plateaus spaced by $\sim e^2/h$. Upper inset: SEM of measured device. The nanotube (arrows) is visible under the SiO_2 and top gates. Lower inset: G as a function of two top gates, with $V_{SD} = 36$ mV. (b) $G(V_{BG})$ at $V_{SD} = 35$ mV for another device, with $d \sim 3.2$ nm. Conductance plateaus appear for both hole (blue trace, bottom axis) and electron (red trace, top axis) transport. Different series resistances have been subtracted from the traces as noted on the figure. (c) G as a function of V_{SD} and top gate voltage at $T = 50$ K for a bent-tube device, $d \sim 4.5$ nm, with a top gate. $R_S = 11.8$ kΩ.

Figure 4 shows the low-bias conductance plateaus of the side-gated device [Fig. 1(b), inset] as a function of temperature and magnetic field. No series resistance has been subtracted from these data. The plateau near e^2/h, which shows considerable overshoot at low temperature, rises to a value close to $1.5e^2/h$ with increasing temperature, while the subsequent plateaus are smoothed with increasing temperature but do not rise significantly. Plateaus measured for

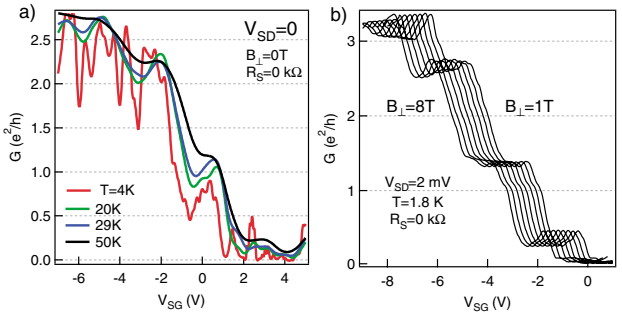

FIG. 4 (color). (a) Temperature dependence of conductance plateaus around $V_{SD} = 0$ for the device in Fig. 1(b) (inset). (b) Evolution of the low-bias conductance plateaus for the same device (different cooldown) in a magnetic field perpendicular to the sample plane with $V_{BG} = 0.68$ V. Curves are offset in V_{SG} for clarity. No series resistance is subtracted in (a) or (b).

this device at high bias show little change with increasing temperature. Magnetic field applied perpendicular to the tube axis has little effect on plateau structure [Fig. 4(b)]. Here, the Zeeman splitting at $B = 8$ T, $g\mu_B B \sim 0.9$ meV, is greater than thermal energy ($k_B T \sim 0.15$ meV) but less than the voltage bias ($eV_{SD} = 2$ meV). Comparable ratios of magnetic field to bias energies induce significant change in $G(V_G)$ curves in GaAs quantum point contacts with spin degenerate levels. Possibly relevant to our results is the appearance of a zero-magnetic-field conductance plateau near e^2/h [26], or more commonly closer to $0.7(2e^2/h)$ [27–29], in gate-defined semiconductor quantum point contacts and wires. A theoretical model of this so-called 0.7 structure in quantum point contacts involving the formation of an ordered electronic state in 1D [30] may be relevant in nanotubes as well. Finally, we note that previous studies of Pd nanowires have observed conductance plateaus at $\sim e^2/h$, which the authors suggested may indicate ferromagnetism or near-ferromagnetism in Pd nanostructures [31] (though $\sim e^2/h$ plateaus were also seen in similar Ti structures). The plateau structure reported here is most evident in Pd-contacted nanotubes; however, we believe this is primarily due to the highly transparent contacts obtained with Pd rather than an effect of near-ferromagnetism in the leads, as magnetic field sweeps at both high field and around zero field showed no hysteresis or change in plateau structure.

The authors wish to thank M. Gershow and D. C. Bell for their help with TEM. This work was supported by NSF-NIRT (EIA-0210736), and ARO/ARDA (DAAD19-02-1-0039 and -0191) and Harvard CIMS. M. J. B. acknowledges support from NSF and ARO-QCGR.

*Permanent Address: Department of Physics, Weizmann Institute, Rehovot, Israel.

[1] T. Ando, T. Nakanishi, and R. Saito, Microelectron. Eng. **47**, 421 (1999).
[2] B. J. van Wees, H. van Houten, C. W. J. Beenakker *et al.*, Phys. Rev. Lett. **60**, 848 (1988).
[3] A. Yacoby, H. L. Stormer, N. S. Wingreen *et al.*, Phys. Rev. Lett. **77**, 4612 (1996).
[4] H. van Houten, C. Beenakker, and B. van Wees, in *Nanostructured Systems*, edited by M. A. Reed (Academic Press, San Diego, 1992), Vol. 35, p. 9.
[5] C. Beenakker and H. van Houten, in *Solid State Physics — Advances in Research and Applications*, edited by H. a. T. Ehrenreich, D. (Academic Press, San Diego, 1991), Vol. 44, p. 1.
[6] T. Ando, Semicond. Sci. Technol. **15**, R13 (2000).
[7] W. Liang, M. Bockrath, and H. Park, Phys. Rev. Lett. **88**, 126801 (2002).
[8] S. Frank, P. Poncharal, Z. L. Wang *et al.*, Science **280**, 1744 (1998).
[9] R. D. Antonov and A. T. Johnson, Phys. Rev. Lett. **83**, 3274 (1999).
[10] J. Appenzeller, J. Knoch, M. Radosavljevic *et al.*, Phys. Rev. Lett. **92**, 226802 (2004).
[11] A. Javey, J. Guo, Q. Wang *et al.*, Nature (London) **424**, 654 (2003).
[12] While we cannot exclude the possibility that our nanotubes are small ropes or double walled tubes, all devices for this study can be fully depleted with the back gate. Therefore, it is likely that only a single semiconducting tube is participating in transport. In addition, using TEM analysis of nanotubes grown under similar conditions we were able to distinguish between large ropes and single tubes. Further, we were unable to observe any internal structure in single tubes with diameters less than ~4 nm.
[13] H. W. C. Postma, T. Teepen, Z. Yao *et al.*, Science **293**, 76 (2001).
[14] D. Bozovic, M. Bockrath, J. H. Hafner *et al.*, Appl. Phys. Lett. **78**, 3693 (2001).
[15] M. J. Biercuk, N. Mason, and C. M. Marcus, cond-mat/0312276 [Nano Letters (to be published)].
[16] N. Mason, M. J. Biercuk, and C. M. Marcus, Science **303**, 655 (2004).
[17] S. J. Wind, J. Appenzeller, and P. Avouris, Phys. Rev. Lett. **91**, 058301 (2003).
[18] W. Liang, M. Bockrath, D. Bozovic *et al.*, Nature (London) **411**, 665 (2001).
[19] L. I. Glazman and A. V. Khaetskii, Europhys. Lett. **9**, 263 (1989).
[20] N. K. Patel, J. T. Nicholls, L. Martin-Moreno *et al.*, Phys. Rev. B **44**, 13549 (1991).
[21] P. L. McEuen, M. Bockrath, D. H. Cobden *et al.*, Phys. Rev. Lett. **83**, 5098 (1999).
[22] We distinguish between this coupling constant and the familiar ''lever arm'' (ratio of gate capacitance to total capacitance), extracted from Coulomb blockade diamonds. The quantity alpha characterizes a change in Fermi energy induced by a gate, in the present case dominated by a change in density.
[23] A. Nojeh, G. W. Lakatos, S. Peng *et al.*, Nano Lett. **3**, 1469 (2003).
[24] Series resistance is presumably dominated by contact resistance at the Pd-nanotube interface. However, back gate-voltage-dependent scattering within the tube away from the gated region may also contribute.
[25] R. Martel, V. Derycke, C. Lavoie *et al.*, Phys. Rev. Lett. **87**, 256805 (2001).
[26] D. J. Reilly, T. M. Buehler, J. L. O'Brien *et al.*, Phys. Rev. Lett. **89**, 246801 (2002).
[27] K. J. Thomas, J. T. Nicholls, M. Y. Simmons *et al.*, Phys. Rev. Lett. **77**, 135 (1996).
[28] S. M. Cronenwett, H. J. Lynch, D. Goldhaber-Gordon *et al.*, Phys. Rev. Lett. **88**, 226805 (2002).
[29] R. de Picciotto, L. N. Pfeiffer, K. W. Baldwin *et al.*, Phys. Rev. Lett. **92**, 036805 (2004).
[30] K. A. Matveev, Phys. Rev. Lett. **92**, 106801 (2004).
[31] V. Rodrigues, J. Bettini, P. C. Silva *et al.*, Phys. Rev. Lett. **91**, 096801 (2003).